ACS OMEGA

http://pubs.acs.org/journal/acsodf

Article

Tuning Chromophore-Based LMOF Dimensionality to Enhance Detection Sensitivity for Fe^{3+} Ions

Fang-Ming Wang,* Lei Zhou, Ever Velasco, Jun-Feng Li, Xiu-Dian Xu, Li-Zhuang Chen,* and Jing Li*

Cite This: *ACS Omega* 2021, 6, 16498−16506

Read Online

ACCESS | Metrics & More | Article Recommendations | Supporting Information

ABSTRACT: Herein, we report the synthesis of two new manganese-based luminescent metal−organic frameworks (LMOFs) $[Mn_{0.5}(tipe)(1,4\text{-ndc})]_n$ (**1**) and $[Mn(tipe)(1,4\text{-ndc})\ (H_2O)\cdot(DMF)_2\cdot(H_2O)_3]_n$ (**2**) [tipe = 1,1,2,2-tetrakis(4-(1*H*-imidazol-1-yl)phenyl)ethene (tipe) and 1,4-ndc = 1,4-naphthalenedicarboxylic acid] constructed from an aggregation-induced emission (AIE) chromophore ligand. Compound **1** can undergo a facile single-crystal-to-single-crystal transformation to form compound **2**, which results in an increase in dimensionality from a two-dimensional (2D) network to a three-dimensional (3D) network. Both compounds demonstrate excellent performance for the solution-phase detection of Fe^{3+} ions through a significant and rapid quench in luminescence emission. Fluorescence titration experiments reveal that compound **2** is more selective toward Fe^{3+} compared to compound **1** because of its 3D stacking mode. The K_{sv} value for compound **2** (32 378 M^{-1}) is twice as large as that for compound **1** (15 854 M^{-1}) for the detection of Fe^{3+} ions. We attribute this significant increase in performance to the increase in dimensionality. In addition, compound **2** demonstrates high selectivity and sensitivity for the detection of Cr^{3+} cations and $Cr_2O_7^{2-}$ anions.

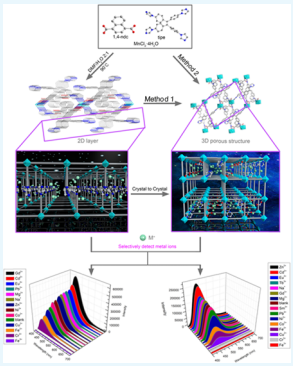

INTRODUCTION

In recent years, chemical sensors have attracted significant attention due to their potential for applications in gas storage and separation, luminescence-based sensing, detection of analytes in the gas or liquid phase, and catalysis, to name a few.[1−6] Luminescence-based detection of harmful analytes is of particular importance due to the general simplicity of the approach. The development of low-cost, portable, precise, and real-time luminescent sensors for the detection of harmful chemical contaminants provides a promising alternative to more resource-intensive detection methods. The rapid detection of heavy metal ions in aqueous systems is of particular importance. Moderate concentrations of metal ions are required in living systems, and various biological disorders may occur from a lack of metal ions, such as Fe^{3+} and Cr^{3+}, in organisms.[7,8] However, high concentrations of metal ions can cause a threat to human health. The use of fluorescent sensors provides a simple technique to selectively detect Fe^{3+} ions.[7,9] Unfortunately, these metal ions coexist in aqueous systems with a wide variety of other metal ions. Thus, the selective fluorescence-based detection of metal ions is of specific interest because materials designed for this purpose need to account for competitive interactions that may occur with other metal ions. In turn, selectively detecting a single metal ion over others can result in an arduous task.

As a family of new porous materials, metal−organic frameworks (MOFs)[10−12] have found significant potential in applications related to chemical sensing, catalysis, gas storage and separation, drug delivery, bioimaging, etc.[13−22] These highly crystalline materials result from the self-assembly of inorganic metal ions with organic linkers into three-dimensional (3D) extended networks. MOFs are endowed with permanent porosity and large surface areas largely attributed to open cavities that remain upon outgassing these materials. The entrance of guest species may be limited by the pore size or aperture of the resulting structure. Among MOFs, luminescent metal−organic frameworks (LMOFs)[23−28] possess outstanding luminescent properties that result after excitation with a light source. Through various types of interactions and mechanisms, guest species that are encapsulated within the pores of these frameworks can result in an enhancement or quenching effect that alters the luminescence of the host, making LMOFs promising candidates for use as chemical sensors.[29−35]

In previous research, we have reported LMOFs for the selective detection of aromatic volatile organic compounds (VOCs) by introducing an organic chromophore that contains the highly fluorescent tetraphenyl ethylene (TPE) core chromophore with an aggregation-induced emission (AIE) effect.[25] Herein, we report two new LMOFs $Mn_{0.5}(tipe)(1,4\text{-ndc})$ (**1, JUST-12 or LMOF-317**) and $[Mn(tipe)(1,4\text{-ndc})(H_2O)]\cdot(DMF)_2\cdot(H_2O)_3$ (**2, JUST-13 or LMOF-318**) based on another TPE-core ligand, 1,1,2,2-tetrakis(4-(1*H*-

Received: March 28, 2021
Accepted: June 1, 2021
Published: June 17, 2021

imidazol-1-yl)phenyl)ethane (tipe)[16] (Figure S1). From a structural perspective, both compounds possess uncoordinated N atoms and O atoms that decorate the walls of the resulting 1D channels and provide open sites for metal ions to interact. Subsequently, we discovered that both materials undergo rapid and selective luminescence quenching when exposed to Fe^{3+} ions. Compound **1** can be used to prepare compound **2** through a two-dimensional (2D) → 3D single-crystal-to-single-crystal transformation.[36,37]

RESULTS AND DISCUSSION

Structural and Topological Analyses. Single-crystal X-ray diffraction (SXRD) studies reveal that **1** crystallizes in the monoclinic system with space group $P2_1/n$ (Table 1). In **1**, every Mn atom takes an octahedral geometry by binding to four N atoms from the imidazolyl groups of four tipe ligands and, in a monodentate fashion, to two O atoms from the carboxylic acid groups of 1,4-ndc. In this structure, the Mn atoms do not form clusters; instead, a primary building unit (PBU) extends the structure into a two-dimensional (2D) net (Figure 1a). The bond distances of Mn−N range from 2.273 to 2.320 Å, and the bond distances of Mn−O are all 2.150 Å (Table S1).[39,40] A closer look at the structure reveals that every tipe molecule within the structure possesses two uncoordinated N atoms and that every 1,4-ndc molecule possesses a single uncoordinated O atom. These uncoordinated atoms lie between the 2D layers and decorate the walls of the pore (Figure 1b). These 2D layers can then pack with one another through weak intermolecular interactions (Figure 1c). The framework was simplified as a 4-c net with Schläfli symbol by Topos Pro[41,42] (Figure 1d). These uncoordinated functional groups within the structure provide an active site for the interaction between the parent framework and the heavy metal ions.

Table 1. Crystallographic Data for 1 and 2

	1	2
empirical formula	$C_{50}H_{35}Mn_{0.5}N_8O_4$	$C_{50}H_{34}MnN_8O_5$
formula weight	839.33	881.79
space group	$P2_1/n$	$P2_1/n$
a (Å)	13.774(12)	18.176(5)
b (Å)	11.863(11)	8.907(3)
c (Å)	25.44(2)	33.063(10)
α (o)	90	90
β (o)	91.679(10)	95.363(4)
γ (o)	90	90
V (Å^3)	4155(6)	5329(3)
Z	4	4
D_c (g/cm^3)	1.342	1.099
μ (mm^{-1})	0.230	0.295
F (000)	1742.0	1820.0
θ range [deg]	1.602−24.309	2.475−24.999
collected reflections	6725	9239
unique reflections	4509	5235
R_1, wR_2 [$I > 2\sigma(I)$]	0.0856, 0.2497	0.0843, 0.2099
R_1, wR_2 [all data]	0.1222, 0.2924	0.1427, 0.2341
GOF	1.033	1.020

Compound **2** crystallizes in the monoclinic system with space group $P2_1/n$ (Table 1). Compared to **1**, each Mn atom is coordinated to three N atoms from the imidazolyl groups of three tipe ligands and, in a monodentate fashion, to three O atoms from carboxylic acid groups of two 1,4-ndc ligands, forming an octahedral coordination environment (Figure 2a). The bond distances of Mn−N and Mn−O range from 2.241 to 2.271 and 2.121 to 2.232 Å, respectively (Table S1). Similar to compound **1**, one uncoordinated N atom of each tipe and one O atom from the carboxylic acid groups of 1,4-ndc ligand lie in the channel of the structure, providing open sites for a possible interaction between the framework and guest species. The adjacent Mn atoms are bridged by the tipe ligands or 1,4-ndc ligands to generate a 3D framework (Figure 2b). Compound **2** has one-dimensional (1D) channels along the crystallographic b-axis with a pore size of 8.3 × 9.8 Å with a 30.3% solvent-accessible volume calculated by Platon (Figure 2c). Simplification of the structure using tipe as a 3-c node, the framework may be seen as a 2-nodal net with (3, 4)-c net with the Schläfli symbol $\{4.8^2.10^3\}$ (Figure 2d).

Optical Properties. The solid-state luminescent properties of both compounds were studied at room temperature (Figure 3a). **1**, **2**, and tipe all exhibit blue emission at 448 nm (397 nm excitation), 478 nm (380 nm excitation), and 455 nm (378 nm excitation), respectively. The luminescent property of these compounds originates from the AIE TPE-core.[16,25,43−45] The Commission International de l'Eclairage (CIE) coordinates of **1**, **2**, and tipe are (0.158, 0.129), (0.174, 0.260), and (0.175, 0.187), respectively (Figure 3b). Upon outgassing the porous structure **2**, we notice a red shift (17 nm) in the emission peak compared to the as-made sample (Figure S2). This indicates that the luminescence of compound **2** may be altered by the guests' species, in this case dimethylformamide (DMF) and water, located within the pores of materials that interact weakly with the organic linker.

Porosity Analyses. The permanent porosity of compound **2** was assessed by N_2 adsorption−desorption experiments conducted at 77 K. The Brunauer−Emmett−Teller (BET) surface area of 276.17 m^2/g was estimated from the nitrogen isotherms. The powder X-ray diffraction (PXRD) pattern of compound **2** remained intact after N_2 isotherms and demonstrated that this material is permanently porous (Figures S3b and S4).

Sensing of Metal Ions. Based on the above structure analysis, the interaction sites and porous nature of **1** and **2** render them as good candidates for luminescence-based sensing of suitable guest molecules. Since the luminescent properties of both compounds may depend on the solvents contained within the pores, we exposed them to various organic solvents to study their stability and change in luminescence (Figures S3 and S5). Samples underwent solvent exchange every 4 h at room temperature for 24 h, and then, **1** and **2** were dispersed through ultrasonication to a concentration of 1 mM for 30 min before collecting fluorescence data. The results indicate that although there exist some minor differences on small peaks caused by solvent effects, frameworks of compounds **1** and **2** are still stable. Also, both compounds experience a luminescence enhancement upon submerging in water (Figure S5). Based on the solvent-stability results, further experiments to detect metal ions were conducted in an aqueous environment. Various metal ion solutions of 1 mM were injected into 10 mM suspensions of MOF samples in water after which the changes in luminescence were recorded at room temperature under 365 nm excitation (Figure 4).

As shown in Figure 4, Fe^{3+} ions quenched luminescence emission of **1** and **2**. For **1** (Figure 4a), the addition of Gd^{3+},

https://doi.org/10.1021/acsomega.1c01148
ACS Omega 2021, 6, 16498−16506

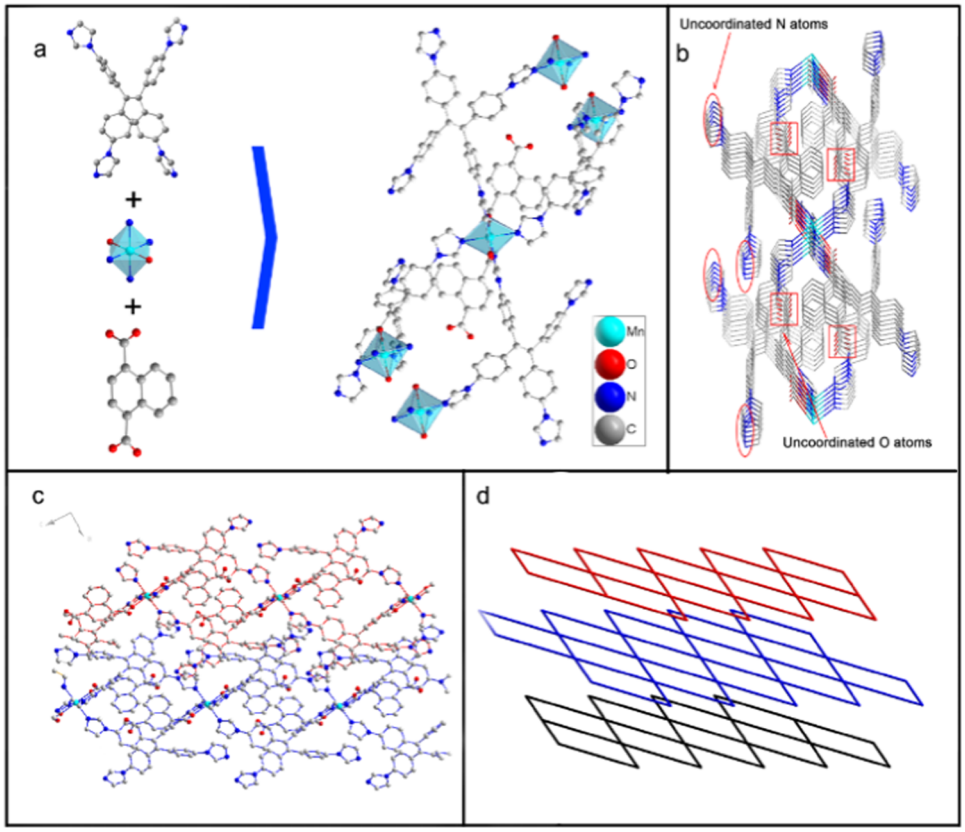

Figure 1. (a) Coordination environment of **1**: Mn atoms connect to four N atoms and two O atoms. (b) Two N atoms from two different imidazolyl groups of each tipe ligand and one O atom from one carboxylic acid group of each 1,4-ndc ligand are uncoordinated. (c) Depiction of the 3D packing of the 2D nets. (d) Topological structure of **1**. The framework was simplified as a 4-c net with Schläfli symbol. In all structures, hydrogen atoms have been omitted for clarity.

Cd^{2+}, Eu^{3+}, Pb^{2+}, Mg^{2+}, Na^{+}, Zn^{2+}, Ni^{2+}, and Co^{2+} ions resulted in a slight enhancement of emission, but the addition results in a slight quench in the case of Cu^{2+}, Fe^{2+}, and Cr^{3+}. As for **2**, the addition of Zn^{2+} and Cd^{2+} results in a slight enhancement in emission, but nearly no obvious spectral changes were recorded in the case of alkali metal cations, such as Na^{+} and Mg^{2+}, and rare-earth metal cations, such as Gd^{3+}, Eu^{3+}, and Sm^{3+}, while Fe^{3+}, Ni^{2+}, Cu^{2+}, and Co^{2+} ions result in a slight quench in emission. Furthermore, after completing the fluorescence detection experiments, both compounds **1** and **2** experience a significant change after exposure to Fe^{3+} and convert to a yellow color within 1 min, indicating the adsorption of the metal ions from the solution. The selectivity toward Fe^{3+} was then tested by placing the compounds with adsorbed Fe^{3+} ions in aqueous solutions of Ni^{2+}, Cu^{2+}, and Co^{2+} for a week (Figures S6 and S7). To our surprise, the compounds both retain their yellow color, indicating that both compounds **1** and **2** prefer to selectively bind the yellow Fe^{3+} ions over other heavy metal ions. To further study the competitive adsorption of heavy metal ions, we introduced samples to multiple equivalents of other metal ions and discovered that the luminescent response induced by Fe^{3+} is not altered, suggesting that **1** and **2** can sense Fe^{3+} with remarkable selectivity. Compared to **1**, **2** also can detect Cr^{3+} ions, though the quenching effect of Fe^{3+} is superior to that of Cr^{3+}. The mechanism of luminescence quenching induced by Fe^{3+} or Cr^{3+} is due to the interaction of Fe^{3+} or Cr^{3+} with the uncoordinated N atom of tipe and O atoms of 1,4-ndc, reducing the efficiency of ligand to metal charge transfer (LMCT).[22]

The quenching effects of anions for **2** were also studied (Figure S8). The result reveals that only $Cr_2O_7^{2-}$ anions completely quench the fluorescence of **2**. Out of the inorganic anions that we tested, HCO^{3-}, NO^{3-}, Br^{-}, SO_4^{2-}, and Cl^{-} all result in a slight enhancement in emission, while ClO_4^{-}, I^{-}, and CO_3^{2-} cause a slight quench in emission.

To evaluate the sensing performance of **1** and **2**, fluorescence titration experiments were performed by monitoring the fluorescent changes induced upon the gradual addition of analytes. As shown in Figures 5 and S9, the luminescent intensities of **1** and **2** decrease gradually with the addition of analytes. The quenching efficiency was quantified using the Stern–Volmer (SV) equation[46−50]

$$I_0/I = K_{sv}[Q] + 1$$

I_o and I are the luminescent intensities of suspensions before and after the addition of analytes, respectively, [Q] is the molar concentration of analytes, and K_{sv} is the quenching constant that was used to quantitatively evaluate the sensing efficiency of the two compounds.

From the Stern–Volmer analysis, we clearly see that the quench in emission of compounds **1** and **2** as a function of the concentration of analytes injected follows a linear relationship. For compound **1**, we calculate the K_{sv} to be 15 854 M^{-1} for Fe^{3+} as deduced from the Stern–Volmer (SV) equation. As for compound **2**, the K_{sv} for Fe^{3+} can be calculated to be 32 378 M^{-1}, which is comparable to those of previously reported

https://doi.org/10.1021/acsomega.1c01148
ACS Omega 2021, 6, 16498−16506

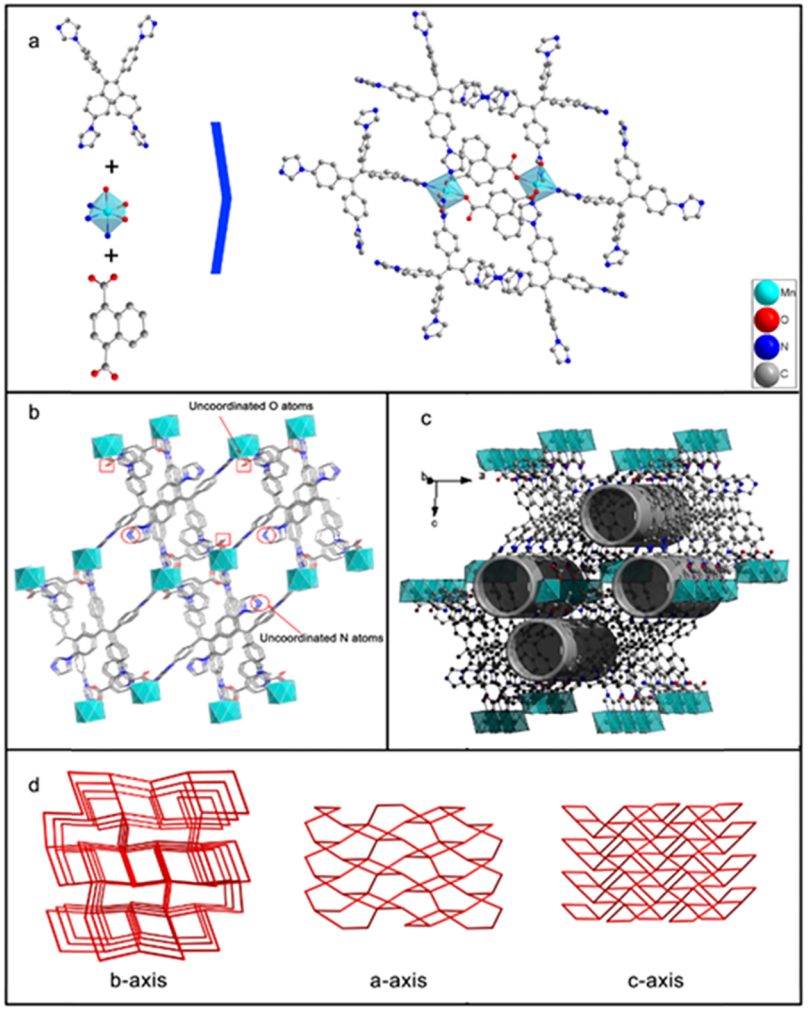

Figure 2. (a) Coordination environment of **2**: Mn atoms connect to three N atoms and three O atoms. (b) One uncoordinated N atom of each tipe and one O atom from the carboxylic acid groups of 1,4-ndc ligand lie in the channel. (c) **2** has 1D channels along the *b*-axis with a pore size of 8.3 × 9.8 Å. (d) Topological structure of **2**. The framework may be expressed as a 2-nodal net (3,4)-c net with Schläfli symbol $\{4.8^2.10^3\}$. In all structures, hydrogen atoms have been omitted for clarity.

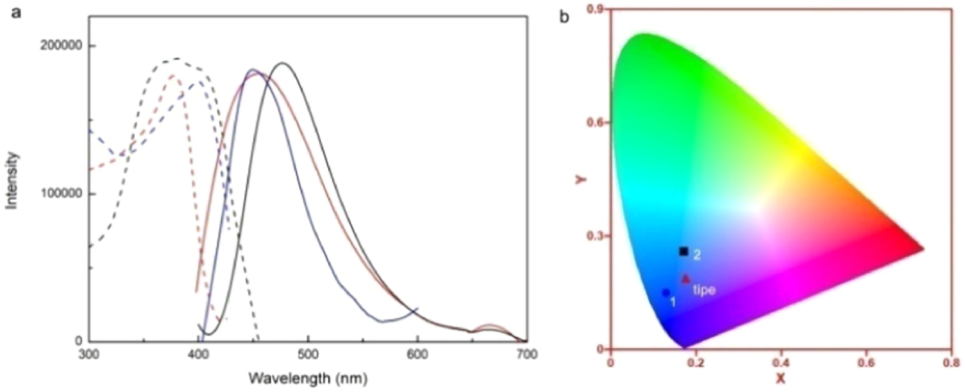

Figure 3. (a) Excitation and emission spectra of **1** (blue), **2** (black), and tipe (red). (b) CIE coordinates of **1** (blue), **2** (black), and tipe (red).

MOF-based sensors for detecting Fe^{3+} and twice as large as for compound **1**. The limit of detection (LOD = $3\sigma/K_{sv}$) values of **1** and **2** were then calculated to be 1.01×10^{-5} M^{-1} and 4.82×10^{-6} M^{-1}, respectively.[51−55] The results indicated that compound **2** has better selectivity toward Fe^{3+} because of its 3D structure. The K_{sv} value for Cr^{3+} was 6258 M^{-1}, half that for Tb($^{3+}$)@Cd-MOF,[56] and the value is far less than that for Fe^{3+}. So, the quenching effect of Fe^{3+} is superior to that of Cr^{3+} remarkably. Fluorescence titration and analysis by the Stern−Volmer equation reveal that compound **2** has a K_{sv} value of 10 113 M^{-1} for $Cr_2O_7^{2-}$, a value comparable to those of materials previously reported for the sensing of Cr^{6+} ions (Figure S9).[53,57]

https://doi.org/10.1021/acsomega.1c01148
ACS Omega 2021, 6, 16498−16506

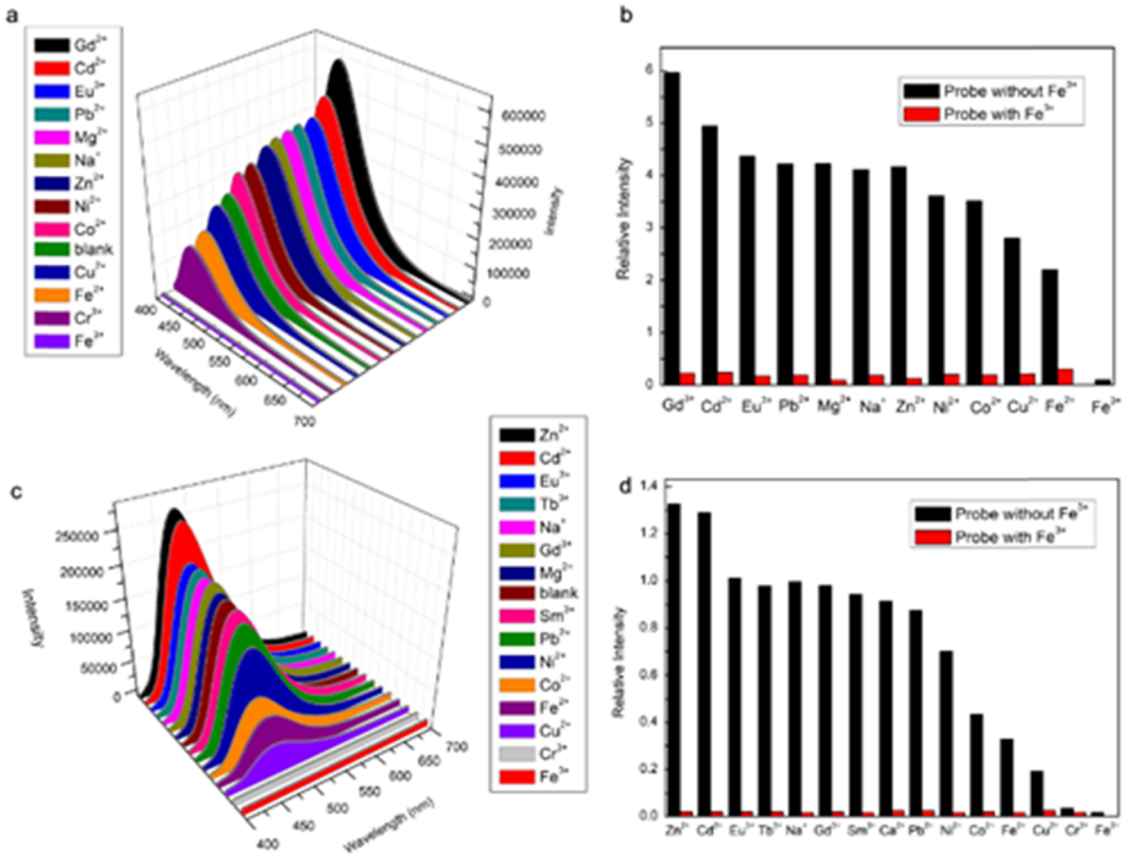

Figure 4. Luminescence spectra of **1** (a) and **2** (c) upon addition of (1 mM) metal ions. Changes in luminescence of **1** (b) and **2** (d) upon addition of Fe^{3+} ions to 1.5 mM.

CONCLUSIONS

In summary, we have successfully prepared two novel manganese LMOFs based on an AIE chromophore ligand, 1,1,2,2-tetrakis(4-(1*H*-imidazol-1-yl)-phenyl)ethane and 1,4-naphthalenedicarboxylic acid. Compound **1** forms a 2D layered structure, while compound **2** forms a 3D extended network. The walls of the resulting pores are decorated with uncoordinated N and O atoms, endowing the materials with an excess of open coordination sites to interact with Fe^{3+} ions. Furthermore, compound **1** can undergo a facile single-crystal-to-single-crystal transformation to convert into compound **2**. The K_{sv} value of compound **2** (32 378 M^{-1}) is double that for compound **1** (15 854 M^{-1}) because of the increase in dimensionality from a 2D to 3D network. Finally, compound **2** also demonstrates high selectivity and sensitivity for Cr^{3+} cations and $Cr_2O_7^{2-}$ anions. These properties make both of these materials good candidates for luminescence-based chemical sensors for the detection of these ions.

EXPERIMENTAL SECTION

Materials and Methods. All reagent-grade chemicals and solvents were obtained from commercial sources and were used without further purification. The luminescence spectra of these compounds were recorded at room temperature on a spectrofluorometer FS5. Powder samples were uniformly coated on quartz slides. Thermogravimetric analyses (TGA) of compounds **1** and **2** were carried out on a TA Q5000 analyzer. Crystal samples were loaded onto a platinum pan and heated at a ramp rate of 15 °C/min from 30 to 800 °C under a nitrogen flow (50 mL/min). Powder X-ray diffraction (PXRD) patterns were recorded on an Ultima IV with Cu Kα radiation (λ = 1.5406 Å). The data was collected at room temperature in the 2θ range of 5−50° with a scan speed of 6°/min and an operating power of 40 kV and 40 mA.

Synthesis of Ligands and Compounds. *Ligand Synthesis.* 1,1,2,2-Tetrakis(4-(1*H*-imidazol-1-yl)phenyl)ethane (tipe) was synthesized as previously reported (Figure S1).[34,38]

*Preparation of $Mn_{0.5}$(tipe)(1,4-ndc) (**1**).* $MnCl_2{\cdot}4H_2O$ (7.9 mg, 0.04 mmol), tipe (5.96 mg, 0.01 mmol), 1,4-naphthalenedicarboxylic acid (1,4-H_2ndc) (4.3 mg, 0.02 mmol), DMF (1 mL), and H_2O (2 mL) were mixed in a 25 mL glass vial and agitated by ultrasonication for 10 min. They were then placed in a preheated oven at 90 °C for 48 h. Colorless crystals of **1** were obtained with a yield of 43% based on tipe. Anal. calcd (%) for $C_{50}H_{35}Mn_{0.5}N_8O_4$: C, 71.55; H, 4.17; N, 13.35. Found: C, 71.42; H, 4.11; N,13.32.

*Preparation of [Mn(tipe)(1,4-ndc)(H_2O)]·$(DMF)_2$·$(H_2O)_3$ (**2**). Method **1**.* Compound **1** (8.4 mg, 0.01 mmol) was added into a 25 mL glass vial with $MnCl_2{\cdot}4H_2O$ (7.9 mg, 0.04 mmol), DMF (1 mL), and H_2O (0.25 mL). The mixture was then heated to 90 °C for 48 h. Yellow rodlike single crystals of **2** were obtained with a yield of 77.5% based on compound **1**. Anal. calcd (%) for $C_{56}H_{56}MnN_{10}O_{10}$: C, 62.05; H, 5.17; N, 12.92. Found: C, 62.08; H, 5.19; N, 12.81.

*Method **2**.* $MnCl_2{\cdot}4H_2O$ (7.9 mg, 0.04 mmol), tipe (5.96 mg, 0.01 mmol), 1,4-naphthalenedicarboxylic acid (1,4-H_2ndc) (4.3 mg, 0.02 mmol), DMF (2 mL), and H_2O (1 mL) were added into a 25 mL glass vial. The resulting suspension was stirred at 90 °C until it became a clear solution; it was then

https://doi.org/10.1021/acsomega.1c01148
ACS Omega 2021, 6, 16498−16506

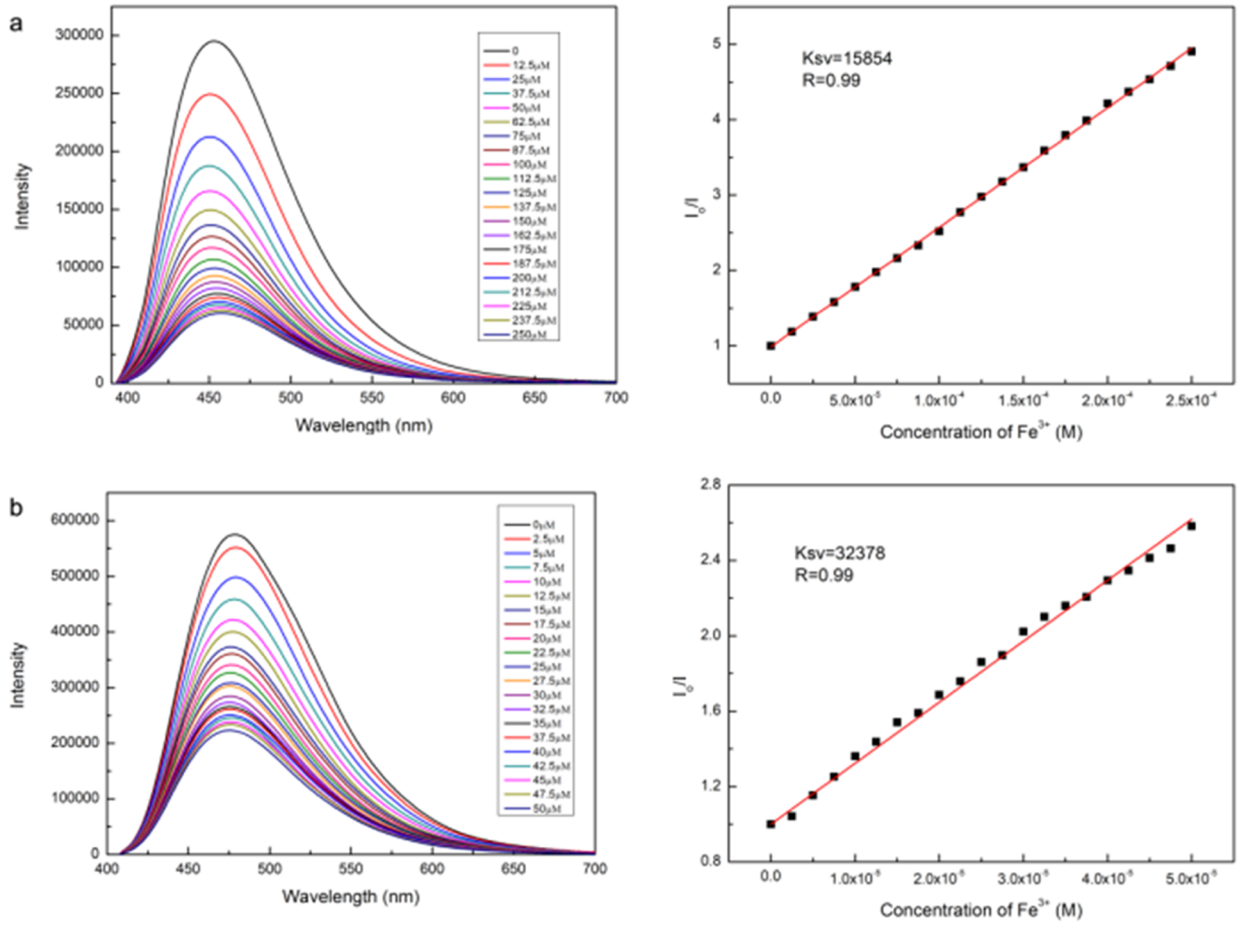

Figure 5. SV curves of **1** (a) and **2** (b) for detecting Fe^{3+}.

Scheme 1. Synthetic Scheme for the Synthesis of Compounds 1 and 2

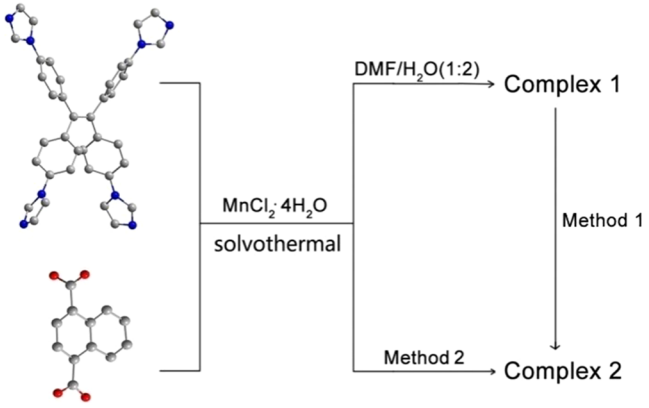

maintained at 90 °C for 48 h to produce yellow rodlike crystals of compound **2** with a yield of 47% based on tipe.

Single-Crystal X-ray Diffraction (SXRD). Single-crystal diffraction data for **1** and **2** were collected using a Bruker SMART APEX II CCD diffractometer with graphite-monochromatic Mo Kα radiation (λ = 0.71073 Å). Data processing, including empirical absorption correction, was performed using SADABS. The structures of **1** and **2** were solved by direct methods and refined by the full-matrix method based on F^2 by means of the SHELXLTL software package. The SQUEEZE routine within the crystallographic program PLATON was employed to treat the disordered solvent molecules in the crystal. Nonhydrogen atoms were refined anisotropically using all reflections with $I > 2\sigma(I)$. All H atoms were placed at the calculated positions (C−H= 0.930 Å for benzene and 0.960 Å for methyl) and refined riding on the parent atoms with U(H) = 1.2 Ueq (bonded C of both benzyl and methyl group atoms) and U(H) = 1.5 Ueq (bonded C of the methyl group). CCDC numbers of **1** and **2** are, respectively, 1588880 and 1539779.

Fluorescence Titration Experiment Details. Fluorescent titration experiments with compounds **1** and **2** were carried out at room temperature to accurately determine their sensing capability toward metal ions. Briefly, approximately 0.01 mmol either compound was well dispersed in 20 mL of water using ultrasonication coupled with vigorous stirring for 30 min. We then transferred a 4 mL portion of this suspension into a quartz cuvette. Aliquots of dissolved heavy metal ion solutions were injected into the quart cuvette with stirring, and after 1 min, fluorescence measurements were collected using a 365 nm excitation wavelength. The concentration ranges of the analytes were 0−250 μM (Fe^{3+}) for 1 and 0−50μM (Fe^{3+}), 0−250μM (Cr^{3+}), and 0−500 μM ($Cr_2O_7^{2-}$) for **2** (Scheme 1).

■ ASSOCIATED CONTENT

Supporting Information

The Supporting Information is available free of charge at https://pubs.acs.org/doi/10.1021/acsomega.1c01148.

https://doi.org/10.1021/acsomega.1c01148
ACS Omega 2021, 6, 16498−16506

^{1}H NMR spectrum of 1,1,2,2-tetrakis(4-(1*H*-imidazol-1-yl)phenyl)ethene (tipe) (Figure S1); solid photoluminescence spectra of **2**′ as-made and degassed samples at room (Figure S2); PXRD of **1** and **2** at 2θ angle of 5−50° (Figure S3); N_2 adsorption−desorption curve of compound **2** with a surface area of 276 m^2/g (Figure S4); fluorescence spectra of **1** and **2** dispersed in different solvents (Figure S5); PXRD of **1** and **2** at 2θ angle of 5−50° after absorbing Fe^{3+}, Co^{2+}, Cu^{2+}, and Ni^{2+} (Figure S6); time-dependent fluorescence spectra of **1** (Figure S7); luminescence spectra of **2** (1 mM) upon adding anions to 10 mM (Figure S8); SV curves of **2** for Cr^{3+} and $Cr_2O_7^{2-}$ (Figure S9); TG curves of **1** and **2** (Figure S10); and selected bond lengths (Å) of **1** and **2** (Table S1) (PDF)

AUTHOR INFORMATION

Corresponding Authors

Fang-Ming Wang − *School of Environmental and Chemical Engineering, Jiangsu University of Science and Technology, Zhenjiang 212003, P. R. China;* orcid.org/0000-0002-9191-3248; Email: wangfmzj@qq.com

Li-Zhuang Chen − *School of Environmental and Chemical Engineering, Jiangsu University of Science and Technology, Zhenjiang 212003, P. R. China;* orcid.org/0000-0001-8582-599X; Email: clz1977@sina.com

Jing Li − *Department of Chemistry and Chemical Biology, Rutgers University, Piscataway, New Jersey 08854, United States;* orcid.org/0000-0001-7792-4322; Email: jingli@rutgers.edu

Authors

Lei Zhou − *School of Environmental and Chemical Engineering, Jiangsu University of Science and Technology, Zhenjiang 212003, P. R. China*

Ever Velasco − *Department of Chemistry and Chemical Biology, Rutgers University, Piscataway, New Jersey 08854, United States*

Jun-Feng Li − *School of Environmental and Chemical Engineering, Jiangsu University of Science and Technology, Zhenjiang 212003, P. R. China*

Xiu-Dian Xu − *School of Environmental and Chemical Engineering, Jiangsu University of Science and Technology, Zhenjiang 212003, P. R. China*

Complete contact information is available at: https://pubs.acs.org/10.1021/acsomega.1c01148

Author Contributions

F.-M.W. conceived the idea, designed the experiments, and finalized the manuscript. L.Z. performed the experiment, analyzed the data, and drafted the manuscript. E.V. revised the manuscript. J.-F.L. and X.-D.X. analyzed the data. L-Z.C. obtained the funding. J.L. obtained the funding. All authors read and approved the final manuscript.

Notes

The authors declare no competing financial interest.

ACKNOWLEDGMENTS

The JUST team aclknowledges the support from the National Natural Science Foundation of China (Grant No. 21671084) and Start-up Foundation and Pre-research Foundation for Natural Science from Jiangsu University of Science and Technology. The RU team acknowledges partial support from the National Science Foundation (Grant No. DMR-1507210).

REFERENCES

(1) Kreno, L. E.; Leong, K.; Farha, O. K.; Allendorf, M.; Van Duyne, R. P.; Hupp, J. T. Metal-organic framework materials as chemical sensors. *Chem. Rev.* **2012**, *112*, 1105−1125.

(2) Hu, Z.; Lustig, W. P.; Zhang, J.; Zheng, C.; Wang, H.; Teat, S. J.; Gong, Q.; Rudd, N. D.; Li, J. Effective Detection of Mycotoxins by a Highly Luminescent Metal-Organic Framework. *J. Am. Chem. Soc.* **2015**, *137*, 16209−16215.

(3) Hao, J.-N.; Yan, B. Ag+-sensitized lanthanide luminescence in Ln3+ post-functionalized metal−organic frameworks and Ag+ sensing. *J. Mater. Chem. A* **2015**, *3*, 4788−4792.

(4) He, Y.-C.; Zhang, H.-M.; Liu, Y.-Y.; Zhai, Q.-Y.; Shen, Q.-T.; Song, S.-Y.; Ma, J.-F. Luminescent Anionic Metal−Organic Framework with Potential Nitrobenzene Sensing. *Cryst. Growth Des.* **2014**, *14*, 3174−3178.

(5) Wenger, O. S. Vapochromism in organometallic and coordination complexes: chemical sensors for volatile organic compounds. *Chem. Rev.* **2013**, *113*, 3686−733.

(6) Lustig, W. P.; Mukherjee, S.; Rudd, N. D.; Desai, A. V.; Li, J.; Ghosh, S. K. Metal-organic frameworks: functional luminescent and photonic materials for sensing applications. *Chem. Soc. Rev.* **2017**, *46*, 3242−3285.

(7) Wang, J.; Jiang, M.; Yan, L.; Peng, R.; Huangfu, M.; Guo, X.; Li, Y.; Wu, P. Multifunctional Luminescent Eu(III)-Based Metal-Organic Framework for Sensing Methanol and Detection and Adsorption of Fe(III) Ions in Aqueous Solution. *Inorg. Chem.* **2016**, *55*, 12660−12668.

(8) Zhao, Y.; Xu, X.; Qiu, L.; Kang, X.; Wen, L.; Zhang, B. Metal-Organic Frameworks Constructed from a New Thiophene-Functionalized Dicarboxylate: Luminescence Sensing and Pesticide Removal. *ACS Appl. Mater. Interfaces* **2017**, *9*, 15164−15175.

(9) Pal, S.; Bharadwaj, P. K. A Luminescent Terbium MOF Containing Hydroxyl Groups Exhibits Selective Sensing of Nitroaromatic Compounds and Fe(III) Ions. *Cryst. Growth Des.* **2016**, *16*, 5852−5858.

(10) Li, H.; Eddaoudi, M.; O'Keeffe, M.; Yaghi, O. M. Design and synthesis of an exceptionally stable and highly porous metal-organic framework. *Nature* **1999**, *402*, 276−279.

(11) O'Keeffe, M.; Yaghi, O. M. Deconstructing the crystal structures of metal-organic frameworks and related materials into their underlying nets. *Chem. Rev.* **2012**, *112*, 675−702.

(12) Cook, T. R.; Zheng, Y. R.; Stang, P. J. Metal-organic frameworks and self-assembled supramolecular coordination complexes: comparing and contrasting the design, synthesis, and functionality of metal-organic materials. *Chem. Rev.* **2013**, *113*, 734−777.

(13) Hu, Z.; Deibert, B. J.; Li, J. Luminescent metal-organic frameworks for chemical sensing and explosive detection. *Chem. Soc. Rev.* **2014**, *43*, 5815−5840.

(14) Lee, J.; Farha, O. K.; Roberts, J.; Scheidt, K. A.; Nguyen, S. T.; Hupp, J. T. Metal-organic framework materials as catalysts. *Chem. Soc. Rev.* **2009**, *38*, 1450−1459.

(15) Li, J. R.; Sculley, J.; Zhou, H. C. Metal-organic frameworks for separations. *Chem. Rev.* **2012**, *112*, 869−932.

(16) Lustig, W. P.; Wang, F.; Teat, S. J.; Hu, Z.; Gong, Q.; Li, J. Chromophore-Based Luminescent Metal-Organic Frameworks as Lighting Phosphors. *Inorg. Chem.* **2016**, *55*, 7250−7256.

(17) Nagarkar, S. S.; Joarder, B.; Chaudhari, A. K.; Mukherjee, S.; Ghosh, S. K. Highly selective detection of nitro explosives by a luminescent metal-organic framework. *Angew. Chem., Int. Ed.* **2013**, *52*, 2881−2885.

(18) Liu, J.; Chen, L.; Cui, H.; Zhang, J.; Zhang, L.; Su, C. Y. Applications of metal-organic frameworks in heterogeneous supramolecular catalysis. *Chem. Soc. Rev.* **2014**, *43*, 6011−6061.

(19) Orcajo, G.; Calleja, G.; Botas, J. A.; Wojtas, L.; Alkordi, M. H.; Sánchez-Sánchez, M. Rationally Designed Nitrogen-Rich Metal−Organic Cube Material: An Efficient CO2 Adsorbent and H2 Confiner. *Cryst. Growth Des.* **2014**, *14*, 739−746.
(20) Wang, H. S. Metal-organic frameworks for biosensing and bioimaging applications. *Coord. Chem. Rev.* **2017**, *349*, 139−155.
(21) Wang, F. M.; Zhou, L.; Lustig, W. P.; Hu, Z. C.; Li, J. F.; Hu, B. X.; Chen, L. Z.; Li, J. Highly Luminescent Metal-Organic Frameworks Based on an Aggregation-Induced Emission Ligand as Chemical Sensors for Nitroaromatic Compounds. *Cryst. Growth Des.* **2018**, *18*, 5166−5173.
(22) Razavi, S. A. A.; Morsali, A. Metal ion detection using luminescent-MOFs: Principles, strategies and roadmap. *Coord. Chem. Rev.* **2020**, *415*, No. 213299.
(23) Cui, Y.; Yue, Y.; Qian, G.; Chen, B. Luminescent functional metal-organic frameworks. *Chem. Rev.* **2012**, *112*, 1126−1162.
(24) Allendorf, M. D.; Bauer, C. A.; Bhakta, R. K.; Houk, R. J. Luminescent metal-organic frameworks. *Chem. Soc. Rev.* **2009**, *38*, 1330−1352.
(25) Wang, F.; Liu, W.; Teat, S. J.; Xu, F.; Wang, H.; Wang, X.; An, L.; Li, J. Chromophore-immobilized luminescent metal-organic frameworks as potential lighting phosphors and chemical sensors. *Chem. Commun.* **2016**, *52*, 10249−10252.
(26) Wang, F.; Zhou, Z.; Liu, W.; Zhou, L.; Chen, L.; Li, J. Two blue-light excitable yellow-emitting LMOF phosphors constructed by triangular tri(4-pyridylphenyl)amine. *Dalton Trans.* **2017**, *46*, 956−961.
(27) Li, X.; Yang, L.; Zhao, L.; Wang, X. L.; Shao, K. Z.; Su, Z. M. Luminescent Metal-Organic Frameworks with Anthracene Chromophores: Small-Molecule Sensing and Highly Selective Sensing for Nitro Explosives. *Cryst. Growth Des.* **2016**, *16*, 4374−4382.
(28) Kaur, H.; Sundriyal, S.; Pachauri, V.; Ingebrandt, S.; Kim, K. H.; Sharma, A. L.; Deep, A. Luminescent metal-organic frameworks and their composites: Potential future materials for organic light emitting displays. *Coord. Chem. Rev.* **2019**, *401*, No. 213077.
(29) Lan, A.; Li, K.; Wu, H.; Olson, D. H.; Emge, T. J.; Ki, W.; Hong, M.; Li, J. A luminescent microporous metal-organic framework for the fast and reversible detection of high explosives. *Angew. Chem., Int. Ed.* **2009**, *48*, 2334−2338.
(30) Douvali, A.; Tsipis, A. C.; Eliseeva, S. V.; Petoud, S.; Papaefstathiou, G. S.; Malliakas, C. D.; Papadas, I.; Armatas, G. S.; Margiolaki, I.; Kanatzidis, M. G.; Lazarides, T.; Manos, M. J. Turn-on luminescence sensing and real-time detection of traces of water in organic solvents by a flexible metal-organic framework. *Angew. Chem., Int. Ed.* **2015**, *54*, 1651−1656.
(31) Huang, R. W.; Wei, Y. S.; Dong, X. Y.; Wu, X. H.; Du, C. X.; Zang, S. Q.; Mak, T. C. W. Hypersensitive dual-function luminescence switching of a silver-chalcogenolate cluster-based metal-organic framework. *Nat. Chem.* **2017**, *9*, 689−697.
(32) Stassen, I.; Burtch, N.; Talin, A.; Falcaro, P.; Allendorf, M.; Ameloot, R. An updated roadmap for the integration of metal-organic frameworks with electronic devices and chemical sensors. *Chem. Soc. Rev.* **2017**, *46*, 3185−3241.
(33) Lim, K. S.; Jeong, S. Y.; Kang, D. W.; Song, J. H.; Jo, H.; Lee, W. R.; Phang, W. J.; Moon, D.; Hong, C. S. Luminescent Metal-Organic Framework Sensor: Exceptional Cd2+ Turn-On Detection and First In Situ Visualization of Cd2+ Ion Diffusion into a Crystal. *Chem. - Eur. J.* **2017**, *23*, 4803−4809.
(34) Ye, J. W.; Zhao, L. M.; Bogale, R. F.; Gao, Y.; Wang, X. X.; Qian, X. M.; Guo, S.; Zhao, J. Z.; Ning, G. L. Highly Selective Detection of 2,4,6-Trinitrophenol and Cu2+ Ions Based on a Fluorescent Cadmium-Pamoate Metal-Organic Framework. *Chem. - Eur. J.* **2015**, *21*, 2029−2037.
(35) Zhao, S. N.; Song, X. Z.; Zhu, M.; Meng, X.; Wu, L. L.; Feng, J.; Song, S. Y.; Zhang, H. J. Encapsulation of Ln(III) Ions/Dyes within a Microporous Anionic MOF by Post-synthetic Ionic Exchange Serving as a Ln(III) Ion Probe and Two-Color Luminescent Sensors. *Chem. - Eur. J.* **2015**, *21*, 9748−9752.
(36) Hu, C.; Englert, U. Crystal-to-crystal transformation from a chain polymer to a two-dimensional network at low temperatures. *Angew. Chem., Int. Ed.* **2005**, *44*, 2281−2283.
(37) Guo, Z. J.; Yu, J.; Zhang, Y. Z.; Zhang, J.; Chen, Y.; Wu, Y.; Xie, L. H.; Li, J. R. Water-Stable In(III)-Based Metal-Organic Frameworks with Rod-Shaped Secondary Building Units: Single-Crystal to Single-Crystal Transformation and Selective Sorption of C2H2 over CO2 and CH4. *Inorg. Chem.* **2017**, *56*, 2188−2197.
(38) Kim, K. Y.; Jung, S. H.; Lee, J. H.; Lee, S. S.; Jung, J. H. An imidazole-appended p-phenylene-Cu(II) ensemble as a chemoprobe for histidine in biological samples. *Chem. Commun.* **2014**, *50*, 15243−15246.
(39) Goswami, S.; Leitus, G.; Goldberg, I. Field-Dependent Magnetic Behaviour in MnII (dicarboxylate)-(bipyridyl)-type 3D Metal-Organic Frameworks with Interpenetrated Structures. *ChemistrySelect* **2017**, *2*, 2322−2329.
(40) He, Y. P.; Yuan, L. B.; Xu, H.; Zhang, J. Control of Interpenetration and Gas-Sorption Properties of Three Mn(II)-tris((4-carboxyl)phenylduryl)amine Frameworks by Tuning Solvent and Temperature. *Cryst. Growth Des.* **2017**, *17*, 290−294.
(41) Blatov, V. A.; Shevchenko, A. P.; Proserpio, D. M. Applied Topological Analysis of Crystal Structures with the Program Package ToposPro. *Cryst. Growth Des.* **2014**, *14*, 3576−3586.
(42) Gunter, M. J.; Hoover, D. R.; Yu, H.; Wassertheil-Smoller, S.; Manson, J. E.; Li, J. X.; Harris, T. G.; Rohan, T. E.; Xue, X. N.; Ho, G. Y. F.; Einstein, M. H.; Kaplan, R. C.; Burk, R. D.; Wylie-Rosett, J.; Pollak, M. N.; Anderson, G.; Howard, B. V.; Strickler, H. D. A prospective evaluation of insulin and insulin-like growth factor-I as risk factors for endometrial cancer. *Cancer Epidemiol., Biomarkers Prev.* **2008**, *17*, 921−929.
(43) Hu, Z.; Huang, G.; Lustig, W. P.; Wang, F.; Wang, H.; Teat, S. J.; Banerjee, D.; Zhang, D.; Li, J. Achieving exceptionally high luminescence quantum efficiency by immobilizing an AIE molecular chromophore into a metal-organic framework. *Chem. Commun.* **2015**, *51*, 3045−3048.
(44) Xu, X. D.; Liang, Y.; Li, J. F.; Zhou, L.; Chen, L. Z.; Wang, F. M. A stable zinc(II)-organic framework as rapid and multi-responsive luminescent sensor for metal ions in water. *J. Coord. Chem.* **2020**, *73*, 867−876.
(45) Xu, X. D.; Liang, Y.; Mensah, A.; Li, J. F.; Zhou, L.; Chen, L. Z.; Wang, F. M. Synthesis, Structures and Fluorescence Properties of Two Novel Cadmium MOFs Based on a Tetraphenylethene(TPE)-Core Ligand. *ChemistrySelect* **2019**, *4*, 12380−12385.
(46) Li, H. H.; Han, Y. B.; Shao, Z. C.; Li, N.; Huang, C.; Hou, H. W.; Water-stable; u-MOF, E. fluorescent sensors for trivalent metal ions and nitrobenzene. *Dalton Trans.* **2017**, *46*, 12201−12208.
(47) Liu, X. G.; Wang, H.; Chen, B.; Zou, Y.; Gu, Z. G.; Zhao, Z.; Shen, L. A luminescent metal-organic framework constructed using a tetraphenylethene-based ligand for sensing volatile organic compounds. *Chem. Commun.* **2015**, *51*, 1677−1680.
(48) Zhang, L.; Kang, Z.; Xin, X.; Sun, D. Metal−organic frameworks based luminescent materials for nitroaromatics sensing. *CrystEngComm* **2016**, *18*, 193−206.
(49) Hu, Z. C.; Tan, K.; Lustig, W. P.; Wang, H.; Zhao, Y. G.; Zheng, C.; Banerjee, D.; Emge, T. J.; Chabal, Y. J.; Li, J. Effective sensing of RDX via instant and selective detection of ketone vapors. *Chem. Sci.* **2014**, *5*, 4873−4877.
(50) Nagarkar, S. S.; Desai, A. V.; Ghosh, S. K. A fluorescent metal-organic framework for highly selective detection of nitro explosives in the aqueous phase. *Chem. Commun.* **2014**, *50*, 8915−8918.
(51) Yan, W.; Zhang, C. L.; Chen, S. G.; Han, L. J.; Zheng, H. G. Two Lanthanide Metal-Organic Frameworks as Remarkably Selective and Sensitive Bifunctional Luminescence Sensor for Metal Ions and Small Organic Molecules. *ACS Appl. Mater. Interfaces* **2017**, *9*, 1629−1634.
(52) Zhao, X. L.; Tian, D.; Gao, Q.; Sun, H. W.; Xu, J.; Bu, X. H. A chiral lanthanide metal-organic framework for selective sensing of Fe(III) ions. *Dalton Trans.* **2016**, *45*, 1040−1046.

https://doi.org/10.1021/acsomega.1c01148
ACS Omega 2021, 6, 16498−16506

(53) Yan, Y. T.; Zhang, W. Y.; Zhang, F.; Cao, F.; Yang, R. F.; Wang, Y. Y.; Hou, L. Four new metal-organic frameworks based on diverse secondary building units: sensing and magnetic properties. *Dalton Trans.* **2018**, *47*, 1682−1692.
(54) Wu, Z. F.; Huang, X. Y. A series of Mg-Zn heterometallic coordination polymers: synthesis, characterization, and fluorescence sensing for Fe(3+), CS2, and nitroaromatic compounds. *Dalton Trans.* **2017**, *46*, 12597−12604.
(55) Gao, M. L.; Wei, N.; Han, Z. B. Anionic metal-organic framework for high-efficiency pollutant removal and selective sensing of Fe(III) ions. *RSC Adv.* **2016**, *6*, 60940−60944.
(56) Wang, Y.; Yang, H.; Cheng, G.; Wu, Y. Y.; Lin, S. M. A new Tb(III)-functionalized layer-like Cd MOF as luminescent probe for high-selectively sensing of Cr3+. *CrystEngComm* **2017**, *19*, 7270−7276.
(57) Guo, X. Y.; Zhao, F.; Liu, J. J.; Liu, Z. L.; Wang, Y. Q. An ultrastable zinc(II)-organic framework as a recyclable multi-responsive luminescent sensor for Cr(III), Cr(VI) and 4-nitrophenol in the aqueous phase with high selectivity and sensitivity. *J. Mater. Chem. A.* **2017**, *5*, 20035−20043.

https://doi.org/10.1021/acsomega.1c01148
ACS Omega 2021, 6, 16498−16506